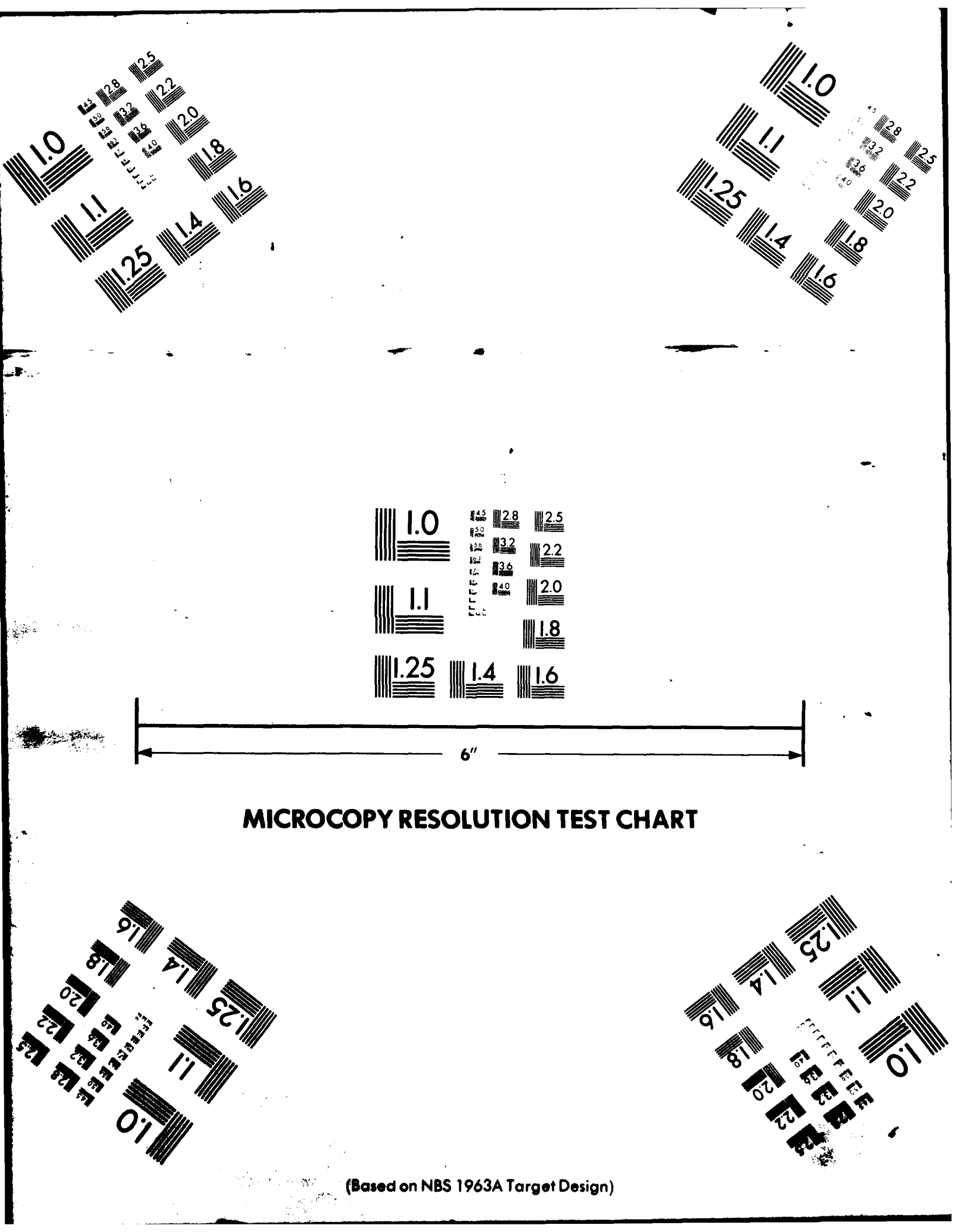

MICROCOPY RESOLUTION TEST CHART

(Based on NBS 1963A Target Design)

NOSC CR 168

Contractor Report 168

LIDAR MEASUREMENTS FOR ASTRONOMICAL REFRACTION

Feasibility and system definition study

Stephen A DeLateur
SRI International
N66001-81-R-0249

February 1983

Final report: 1 April — 30 September 1981

Prepared for
Naval Material Command

NAVAL OCEAN SYSTEMS CENTER
San Diego, California 92152

NAVAL OCEAN SYSTEMS CENTER, SAN DIEGO, CA 92152

AN ACTIVITY OF THE NAVAL MATERIAL COMMAND

JM PATTON, CAPT, USN
Commander

HL BLOOD
Technical Director

ADMINISTRATIVE INFORMATION

Work was performed by SRI International, Menlo Park, California, for NOSC Environmental Sciences Department under contract N66001-81-R-0249, project element 62759, project EP33, task SF59551697.

Released by
JH Richter, Head
Ocean and Atmospheric
Sciences Division

Under authority of
JD Hightower, Head
Environmental Sciences
Department

ACKNOWLEDGEMENTS

The author thanks JA Hughes of the U.S. Naval Observatory in Washington, D.C., for his helpful discussions and aid during the project. Also, the support of JH Richter of the Naval Ocean Systems Center, San Diego, California, is greatly appreciated.

UNCLASSIFIED

SECURITY CLASSIFICATION OF THIS PAGE (When Data Entered)

REPORT DOCUMENTATION PAGE		READ INSTRUCTIONS BEFORE COMPLETING FORM
1. REPORT NUMBER NOSC Contractor Report 168 (CR 168)	2. GOVT ACCESSION NO.	3. RECIPIENT'S CATALOG NUMBER
4. TITLE (and Subtitle) LIDAR MEASUREMENTS FOR ASTRONOMICAL REFRACTION Feasibility and System Definition Study		5. TYPE OF REPORT & PERIOD COVERED Final report 1 April 1981–30 September 1981 6. PERFORMING ORG. REPORT NUMBER
7. AUTHOR(s) Stephen A. DeLateur SRI International		8. CONTRACT OR GRANT NUMBER(s) N66001-81-R-0249
9. PERFORMING ORGANIZATION NAME AND ADDRESS SRI International 333 Ravenswood Ave Menlo Park, CA 94025		10. PROGRAM ELEMENT, PROJECT, TASK AREA & WORK UNIT NUMBERS 62759, EP33, SF59551697
11. CONTROLLING OFFICE NAME AND ADDRESS Naval Material Command Washington, DC 20360		12. REPORT DATE February 1983 13. NUMBER OF PAGES 44
14. MONITORING AGENCY NAME & ADDRESS(if different from Controlling Office) Naval Ocean Systems Center San Diego, CA 92152		15. SECURITY CLASS. (of this report) Unclassified 15a. DECLASSIFICATION/DOWNGRADING SCHEDULE

16. DISTRIBUTION STATEMENT (of this Report)

Approved for public release; distribution unlimited.

17. DISTRIBUTION STATEMENT (of the abstract entered in Block 20, if different from Report)

18. SUPPLEMENTARY NOTES

19. KEY WORDS (Continue on reverse side if necessary and identify by block number)

20. ABSTRACT (Continue on reverse side if necessary and identify by block number)

Recent improvements in mechanical and optical instrumentation precision have occurred. Therefore, the removal of meteorologically caused systematic errors is now a major consideration in stellar position accuracy and in the repeatability of arrangement in positions taken during nightly observations. The two problems singled out in this report are absolute water vapor content and temperature structure measurements. The study revealed that (1) estimates of water vapor distribution with an accuracy of approximately 20 percent would routinely correct position errors of 0.01 of angle and (2) that knowledge of the temperature structure with an accuracy of 0.5K would remove

(Continued on reverse side)

DD FORM 1 JAN 73 1473 EDITION OF 1 NOV 65 IS OBSOLETE

S N 0102-LF-014-6601

UNCLASSIFIED

SECURITY CLASSIFICATION OF THIS PAGE (When Data Entered)

20. Continued

the systematic errors caused by isopycnic tilts, which range from 0.01 up to 0.1 of angle at extreme zenith viewing angles.

The study showed that a remote-sensing solution to the measurement problems of the US Naval Observatory in Washington, DC, is provided by LIDAR (Light Detection and Ranging). Two major LIDAR systems that fulfill the Observatory's needs are based on Raman and DIAL (Differential Absorption Lidar) techniques. We designed a vertical-pointing, conical-scan LIDAR instrument that could measure the layered structure of water vapor density and temperature.

A study and review of experimental systems using the DIAL and Raman techniques indicate that a DIAL system is the recommended approach for simultaneous measurement of water vapor density and temperature. A DIAL system should be constructed to obtain ground-based vertical water vapor and temperature measurements. Further, alexandrite should be used as the lasing medium for the LIDAR system. A breadboard should be constructed with two alexandrite lasers; the primary goals for the breadboard system should be: (1) characterization lasers and (2) application and subsequent analysis of the DIAL techniques for obtaining water vapor profiles. A DIAL technique using three wavelengths near 735 nmi is the recommended approach for the simultaneous measurement of water vapor density and temperature.

CONTENTS

ILLUSTRATIONS

TABLES

I INTRODUCTION AND BACKGROUND

The U.S. Naval Observatory in Washington, D.C., supplies an atlas of the absolute positions of celestial bodies to within .01 seconds of angle for astronomical research and navigation. (These are fundamental measurements; the relative positions of other heavenly bodies are not used.) A major technique used for this work is Transcircle Observation. Employing a combination of the Transit Circle Telescopic instrument with integral north-south pivoting and the earth's east-west rotation during observations allows full-sky coverage.

A. Problem Description

Within the last few years, improvements in instrumentation precision (both mechanical and optical) have led to the realization that the removal of systematic errors due to meteorological causes (often with large spatial and temporal variations) is a major consideration in stellar position accuracy and in the repeatability of the arrangement of positions taken during different nightly observations. The effects of the atmosphere tend to be site-specific, and perhaps, include seasonal variations. Thus, attempts to handle the variation in measured positions with multiple sightings from the same observatory location and then "averaging" the error to reduce its magnitude will not improve the systematic influence on the error structure of the estimates.

Although each major atmospheric constituent can affect viewing the stars, two major areas have been singled out as having the highest priority (see the Appendix). The first is water vapor content along the viewing path. Water vapor changes the gas constant and refractivity values (from those measured and used when assuming dry air). Presently, the ground-level value of the partial pressure of water and a theoretical model for the decrease in water vapor density with altitude are used to compensate for the optical bending applied to the viewing data. An estimate of the actual water vapor distribution with an accuracy of approximately 20 percent would routinely correct position errors of .01 seconds of angle. For those worst-case situations where the existing structure grossly deviates from the linear model, errors approaching .1 seconds of angle could be corrected.

The second problem involves isopycnic tilts (layers of equal atmospheric density). An atmospheric model that entails the existence of concentric spheres of equal density layers is incorrect and leads to errors in position when applied to refraction models, especially when viewing at slant angles instead of directly overhead. The tilt (from exactly concentric) is typically a few degrees. Assuming that isotherms (lines of constant temperature) follow isopycnics, planes of constant

temperature can be measured to specify the degree of tilt along the viewing path. Thus, knowing the temperature structure with an accuracy of .5°K would remove the systematic errors caused by this effect, which range from .01 up to .1 seconds of angle at extreme zenith viewing angles. Because of the precision needed in atmospheric modeling used by the correction algorithms, absolute measurements of the temperature and water vapor content are far more useful than relative measurements.

B. Lidar as a Solution

Lidar (Light Detection and Ranging) provides a remote-sensing solution to the measurement problems of the Observatory. Since the measurements are a set of planes at different heights (to a maximum of 5 km), three-dimensional coverage with a conical scan lidar is necessary. A plane can be defined by measurements taken at different positions at the same altitude. The approach is similar to conventional radar, except the interactions occur at optical frequencies. With a pulsed laser transmitter emitting a narrow, well-collimated beam, and a receiver system (tuned to respond to a specific set of optical wavelengths) positioned at a common location, a telescopic optical receiver can perform ranging by calculating the time for a pulse of radiation to travel the distance to a region of interest plus the time for the backscattered pulse to return. By sampling the time-varying received optical intensity after a specific delay, study of a restricted location along the path can be accomplished.

The lidar system should be a mobile unit so measurements could be obtained at other observatory locations, and for greatly increasing its value as a general development tool.

For most of the compensation programs used at the Naval Observatory, a complete atmospheric profile derived once an hour is sufficient. The profiles should be measured and collected by an integral data collection computer system with storage capability (magnetic tape is the most useful) for post-measurement analysis.

A final requirement and consideration is that operation during the daytime should not be excluded. Although not a major requirement, important position measurements can be taken during daylight hours.

II APPROACH

Two laser systems, each using different physical principles, can supply the atmospheric data needed by the Naval Observatory. The first is Raman Lidar; the second, Differential Absorption Lidar, or DIAL (Hinkley, 1976). This section will briefly describe each system.

A. Raman Lidar

This system transmits a single wavelength, λ_T, and measures the backscattered energy received at up to three other wavelengths, λ_{R1}, λ_{R2}, and λ_{R3}, all different and uniquely Raman-shifted (from the transmitted wavelength) by the molecular species of interest (Cooney, 1970). The amount of backscatter received is proportional to the Raman backscatter coefficient for the molecule being excited at the transmitted wavelength. Figure 1 shows the change in backscatter from nitrogen as the ambient temperature varies. Temperature estimates are calculated by comparing the differential backscatter measurements at λ_{R1} and λ_{R2} for a change in temperature, $\Delta T = T_2 - T_1$. Only the relative temperature differential between two heights can be directly obtained. By measuring the relative backscatter strength from water vapor at λ_{R3}, the relative number density of water vapor-to-nitrogen can be evaluated.

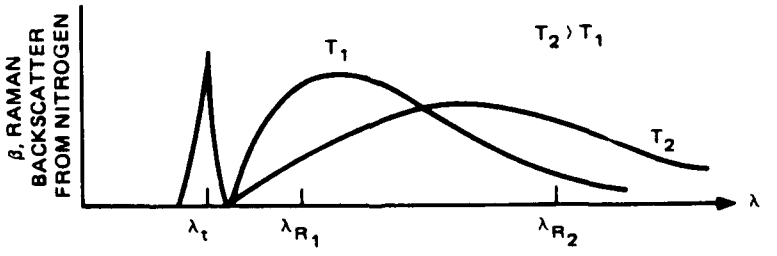

FIGURE 1 TEMPERATURE DEPENDENCE OF RAMAN BACKSCATTER FROM NITROGEN AS A FUNCTION OF WAVELENGTH

B. DIAL Lidar

A DIAL lidar system transmits at least two wavelengths, λ_{T1} and λ_{T2}, tuned to correspond to an absorption line of the species of interest, the "on" wavelength, and to a nonabsorbing region, the "off" wavelength. (Measurement techniques for temperature include a third "on" wavelength.) The receiving system measures the elastic backscattered intensity at each of the transmitted wavelengths, i.e. $\lambda_{R1} = \lambda_{T1}$ and $\lambda_{R2} = \lambda_{T2}$. Backscatter is due to gaseous molecular components (Rayleigh) and to aerosol content (Mie) (Browell et al., 1981; Shotland, 1974).

The ratio in the magnitudes of the returned signals at the "on" and "off" wavelengths can be inverted to yield a concentration estimate. A temperature estimate is obtained by using another "on" wavelength, λ_{T3}. By analyzing the variation of the change in absorption strength with respect to temperature at the two "on" wavelengths, the absolute temperature can be measured. The selection of the "on" absorption region is a tradeoff between choosing a line of sufficient line strength such that the differential measurements can be obtained with sufficient signal-to-noise qualities, and yet not have the absorption of the transmitted laser energy be so great as to prevent enough backscattered signal to be received from the maximum desired range. Section III.C details this technique; Section III.D describes transmission characteristics at 735 nm, an optimum wavelength region for laser transmission.

C. Water Vapor Profiling Systems

Both the Raman and DIAL lidar techniques have successfully demonstrated vertical water vapor density measurements. Significant experiments that have supplied vertical profiles are reviewed in Tables 1 and 2. Those systems that obtained a column-integrated measurement or an average value for a horizontal path were excluded.

Table 1 lists Raman lidar systems that have performed vertical water vapor profiling. All these experiments measure the ratio of the number desity of water vapor to that of nitrogen. Thus, only a water vapor mixing ratio is estimated. (This can be translated into an absolute water vapor density profile by assuming a model density profile for nitrogen with accompanying error.)

Table 2 lists DIAL systems for vertical water vapor profiling Less powerful laser transmitters are needed than those used in Raman-based systems because the Rayleigh-Mie backscatter cross sections are many orders of magnitude larger than Raman cross sections. (Note that the DIAL systems have been operated during the daytime, whereas Raman systems have been limited to night operation only.)

Table 1

RAMAN LIDAR SYSTEMS FOR VERTICAL WATER VAPOR PROFILING

Cooney (1970)

Transmitter: Doubled ruby at 347.15 nm.

Receiver: 397.5 nm from H_2O and 377.7 nm from N_2.

Approach: Water vapor profiles obtained by normalizing H_2O Raman return with N_2 return and assuming an N_2 atmospheric vertical model content.

Accuracy: 13 %.

Range: 300 m - 2600 m with 100-m intervals.

Nighttime measurement.

Melfi (1972)

Transmitter: Doubled ruby at 347.15 nm.

Receiver: 397.5 nm from H_2O and 377.7 nm from N_2.

Approach: Water vapor profile from H_2O return normalized by N_2 return.

Range: 200 m - 2500 m with 50-m intervals.

Nighttime measurement.

Pourny, Renault, and Orszag (1979)

Transmitter: Doubled ruby at 347.15 nm.

Receiver: 397.6 nm from H_2O and 377.7 nm from N_2.

Approach: Water vapor mixing ratio from H_2O return normalized by N_2 return.

Accuracy: 15%

Range: 300 m - 1800 m with 30-m intervals.

Nighttime measurement.

Renault, Pourny, and Capitini (1980)

Transmitter: Quadrupled YAG at 366 nm.

Receiver: 277.5 nm from O_2, 283.6 nm from N_2, and 294.6 nm from H_2O.

Approach: Water vapor mixing ratio from the H_2O return and is normalized by the N_2 return. Estimation of ozone concentration is used to compensate for heavy ozone attenuation of the signals in this wavelength region.

Accuracy: 10% at 500 m with 30-m intervals.

Range: 150 m - 950 m with 30-m intervals.

Daytime operation.

Table 2

DIAL LIDAR SYSTEMS FOR VERTICAL WATER VAPOR PROFILING

Browell, Wilkerson, and McElrath (1979)

Transmitter: Ruby at 694.3 nm and dye (pumped by ruby) at 724.3 nm.

Receiver: 724.3 nm (water vapor absorbing wavelength) and 694.3 nm.

Approach: Difference in returned signals is analyzed for H_2O density profile (mol/cm^3). Equipment includes an absorption cell that measures the cross section for H_2O at the dye laser output for each pulse.

Accuracy: 9%.

Range: 100 m - 3000 m with 100- to 180-m intervals.

Nighttime operation.

Cahen, Pelon, Flamant, Lefere, Chanin, and Megie (1980) and Cahen and Lesne (1981)

Transmitter: Nd:YAG at 532 nm and dye (pumped by Nd:YAG) at 723 nm.

Receiver: 723 nm (absorption by water vapor) and 532 nm.

Approach: Different returns to obtain water vapor profiles. Wavelength and line width of transmitters are servo-controlled.

Accuracy: 10%.

Range: 8000 m with 30-m intervals.

Daytime operation.

Werner and Herrmann (1981)

Transmitter: Ruby at 694.28 nm and temperature-varied ruby from 694.20 nm to 694.28 nm.

Receiver: 694.215 nm (absorbed by water vapor) and 694.237 nm.

Approach: Difference returns to obtain water vapor density profiles.

Accuracy: ± mbar in absolute humidity.

Range: 450 m - 1500 m with 100-m intervals.

Daytime operation.

D. Temperature-Profiling Systems

Table 3 contains a list of the Raman lidar systems for vertical temperature profiling. Common to these experiments is the technique of measuring the temperature dependence in the magnitude of the Raman spectrum of oxygen and nitrogen. The lines in the Raman spectrum for these molecules have differential changes in magnitude with respect to temperature. Thus, by comparing the differential change in two bands, a temperature value can be obtained.

There is a lack of DIAL vertical temperature profiling systems; however, work is presently being performed with techniques that use water vapor lines. One approach is to use "Mason's Method" with the absorption spectra of water vapor in the region of 735 nm (see Section III.C). This wavelength is close to those used for successful DIAL water vapor measurements (724 nm) and other temperature techniques using the absorption spectra of oxygen (760 nm) (Kalshoven et al., 1981). Part of the interest in the area has been generated by the introduction of a tunable solid-state alexandrite laser that has direct application for study in this wavelength region (see Section III.D).

Table 3

RAMAN LIDAR SYSTEMS FOR VERTICAL TEMPERATURE PROFILING

Cooney and Pina (1976)

Transmitter: Ruby at 694.3 nm.

Receiver: 689.0 nm and 691.2 nm.

Approach: Measure the difference in the magnitudes of the Raman spectrum of O_2 and N_2 in two bands which vary with temperature.

Accuracy: 5°C.

Range: 600 m - 1100 m with 300-m intervals.

Nighttime operation.

Gill, Geller, Farina, and Cooney (1979)

Transmitter: Ruby at 694.3 nm.

Receiver: 691.5 nm and 689.0 nm.

Approach: Raman spectrum of O_2 and N_2.

Accuracy: .85°C.

Range: 1300 m - 2300 m with 75-m intervals.

III ANALYSIS

Our evaluation of the capabilities of each lidar technique (DIAL versus Raman) as well as evaluations by other researchers (Wright et al., 1974; Hake et al., 1977) indicate that a DIAL system should be directly applied to the measurements needed by the Observatory. The DIAL technique has demonstrated sensitivity for water vapor content profiling and can be designed to provide sufficient atmospheric temperature structure information during daytime operation.

The study of the DIAL technique involves the use of absorption spectra for constituent and trace gases in the atmosphere and numerical models for the transmission of optical beams through the atmosphere. Research and the collection of experimental and theoretical data by the Air Force Geophysics Laboratory (AFGL) have provided widely recognized code (computer programs) on optical propagation (McClatchey et al., 1970). To use this compendium for numerical analysis in optical propagation, code that describes the absorption of laser lines in the atmosphere had to be converted from the computer language Fortran IV for Control Data Corporation computers to Fortran 77, compatible code for use on the Digital Equipment Corporation VAX 11/782 installed at SRI International.

A. Absorption Spectra Compilation

The absorptic spectra is supplied on two magnetic tapes available from AFGL. One is called the Major Constituents Compilation (Rothman, 1980; McClatchey, 1973); the other is the Trace Gas Compilation (Rothman et al., 1981). Files on the major constituents' tapes contain the molecular transitions of the seven major gases in the atmosphere:

- Water vapor
- Carbon dioxide
- Nitrous oxide
- Carbon monoxide
- Methane
- Oxygen
- Ozone.

The total number of absorptions lines is over 159,000, with the spectra ranging from .3 to 17,880 cm^{-1} (560 nm).

The absorption lines of 13 trace gases are collected in a separate atlas; these include:

- Nitric oxide
- Sulfur dioxide
- Nitrogen dioxide
- Ammonia
- Nitric acid
- Hydroxyl radical
- Hydrogen halides (HF, HCl, HBr, HI)
- Chlorine monoxide
- Carbonyl sulfide
- Formaldehyde.

In the study of the DIAL technique for water vapor and temperature measurement, particular attention was paid to the 700- to 800-nm region in the infrared spectrum where numerous water vapor transitions exist. This is also a spectral region relatively free of absorption lines from other molecules.

B. Computer Codes

The computer program FSCDATM represents the earth's atmosphere as layers in thermal equilibrium. A number of atmospheric model profiles can be chosen as input:

- Tropical atmosphere
- Midlatitude summer or winter
- Subarctic summer or winter
- U.S. 1962 standard.

The user of the code specifies the wavelength region of interest and the geometry of the transmission path, the altitude of transmitter and receiver, and the slant angle between them. The code then outputs a layered model of the atmosphere giving the total density, the average temperature, and the molecular column densities for each layer. The layer thickness is varied according to the user-specified maximum temperature difference between layers. (The layer temperature differential directly affects the computation speed and required accuracy of the absorption calculations.)

The derived model for the atmosphere and the path geometry are then input to the code FASCOD1-Fast Atmospheric Signature Code (Smith et al., 1978). This code performs a line-by-line absorption calculation using a Voight lineshape, a combination of Lorentian (pressure) broadening that best describes transitions in the lower atmosphere; and Doppler (velocity) broadening, with .01 cm^{-1} accuracy (Clough and Kneizys, 1979). All the lines from the seven atmospheric molecules and the 13 trace

bases within the wavelength region of interest are applied in the layer-by-layer calculation.

The total path transmission is obtained by first obtaining the layer parameters from FSCDATM. FASCOD1 then calculates the absorption for each layer, merges the absorption results for all layers, and convolves the derived atmospheric absorption with a modeled instrument transmission function. (Specific laser lines can be calculated by assuming a zero bandwidth for the laser source.)

In the next section we describe a DIAL technique where the transmission characteristics of water vapor absorption lines can measure range-resolved values of water vapor density and temperature simultaneously. Section III.D contains results of transmission simulations that verify this technique.

C. A DIAL Technique for Simultaneous Water Vapor and Temperature Measurements

This approach uses three wavelengths: λ_o, λ_1, and λ_2, where λ_o is located in a nonabsorbing part of the water vapor spectrum, and λ_1 and λ_2 are located at the center of two absorption lines of water vapor with similar absorption coefficients but different line strength sensitivities with respect to temperature (Endemann and Byer, 1981; Endemann and Byer, 1980; Lebow et al., 1982; Rosenberg and Hogan, 1981). (See Section III.D for examples of three wavelengths near 734 nm.)

A DIAL operation is performed with the pairs (λ_o, λ_1) and (λ_o, λ_2). The difference in the optical depth, τ, for one pair of lines over a range cell ΔR at range R can be written as:

$$\tau_1 - \tau_o = \ln\left[\frac{P_1(R)}{P_1(R+\Delta R)}\right] - \ln\left[\frac{P_o(R)}{P_o(R+\Delta R)}\right]$$

$$= 2N(R)\sigma_1\Delta R \quad , \quad \text{(Hinckley, 1976)} \qquad (1)$$

where N(R) is the average water vapor number density over the cell ΔR, and σ_1 is the differential absorption coefficient for wavelengths λ_o and λ_1. Atmospheric backscatter and attenuation caused by scattering (gaseous and particulate) and absorption by other species besides water vapor are assumed to have low spectral variability at the two wavelengths. A similar equation can be written for the second pair of wavelengths, (λ_o, λ_2):

$$\ln\left[\frac{P_2(R)}{P_2(R+\Delta R)}\right] - \ln\left[\frac{P_o(R)}{P_o(R+\Delta R)}\right] = 2N(R)\sigma_2\Delta R \quad . \tag{2}$$

The differential absorption coefficient is a function of the pressure and temperature at the range R. It is defined as

$$\sigma(T,P) = \frac{S(T)}{\pi\ \alpha(T,P)} \quad , \tag{3}$$

where S(T) is the line intensity and $\alpha(T,P)$ is the line halfwidth. In general, the temperature dependence for the line intensity from a nominal temperature, T_o = 296 K, is written as

$$S(T) = S(T_o) \cdot \frac{Q_v(T_o)}{Q_v(T)} \cdot \frac{Q_r(T_o)}{Q_r(T)} \cdot \exp\left[\frac{E}{k}\left(\frac{1}{T_o} - \frac{1}{T}\right)\right]$$

(McClathy, 1973) , (4)

where Q_v is the vibrational partion function; for water vapor Q_v = 1. Q_r is the rotational partition function; for water vapor $Q_r(T) = (T/T_o)^{3/2}\ Q_r(T_o)$. E is the energy of the lower state for the transition, and k is Boltzman's constant. Then,

$$S(T) = S(T_o)[T(R)/T_o]^{-3/2} \exp\left\{\frac{E}{k}\left[\frac{1}{T(R)} - \frac{1}{T_o}\right]\right\} \quad . \tag{5}$$

For the lower atmosphere, the halfwidth temperature and pressure dependence is

$$\alpha(T,P) = \alpha(T_o,P_o)\ [T_o/T(R)]^n\ (P/P_o) \quad , \tag{6}$$

where P_o is a standard pressure for measurements, 1 atm = 1016 mbar, and n is an exponential temperature factor that is modeled as having a value of .5.

The DIAL equation, Eq. (1), can then be rewritten explicity to show the temperature dependence:

$$\ln\left[\frac{P_1(R)/P_1(R+\Delta R)}{P_o(R)/P_o(R+\Delta R)}\right] = 2N(R)\Delta R \cdot$$

$$\frac{S_1(T_o)}{\alpha_1(T_o)}\ \frac{1}{\pi}\left[\frac{T_o}{T(R)}\right]\ \frac{P_o}{P} \exp\left\{\frac{E_1}{k}\left[\frac{1}{T_o} - \frac{1}{T(R)}\right]\right\} \quad . \tag{7}$$

Let $P(R+\Delta R)/P(R)$ be defined as the transmittance, $T(\Delta R)$, through the cell ΔR. Then,

$$\ln\left[\frac{T_o(\Delta R)}{T_1(\Delta R)}\right] = 2\,N(R)\Delta R \quad , \tag{8}$$

with a second similar equation for the other pair of wavelengths. An expression for the average temperature in the range cell can be written by equating the derived number density N(R) for each pair of wavelengths:

$$\frac{\ln[T_o/T_1]}{\ln[T_o/T_2]} = \frac{S_1(T_o)/\alpha_1(T_o)}{S_2(T_o)/\alpha_2(T_o)} \frac{\exp\,[E_1/kT_o]\,\exp\,[-E_1/kT]}{\exp\,[E_2/kT_o]\,\exp\,[-E_2/kT]} \quad . \tag{9}$$

Solving for T(R),

$$T(R) = \left(\frac{E_2 - E_1}{k}\right)\left(\ln\left[\frac{\ln\,[T_o(\Delta R)/T_1(\Delta R)]}{\ln\,[T_o(\Delta R)/T_2(\Delta R)]}\right] - \ln\left[\frac{C_1}{C_2}\right]\right)^{-1} \quad . \tag{10}$$

C_1 and C_2 are constants related to the absorption lines at λ_1 and λ_2, and can be evaluated using line compilation tables (e.g., McClatchey, 1973) or laboratory measurements (Wilkerson et al., 1979), i.e.,

$$C_i = [S_i(T_o)/\alpha_i(T_o)]\,\exp\,[E_i/kT_o)] \quad . \tag{11}$$

Thus, by measuring the transmittance through a range cell ΔR at three wavelengths, $T_o(\Delta R)$, $T_1(\Delta R)$, and $T_2(\Delta R)$, the average temperature for the cell T(R) can be calculated.

After obtaining the temperature for the range cell, the water vapor number density can be calculated from the transmittance difference of either of the line pairs. For (λ_o,λ_1),

$$N(R) = \ln\left[\frac{T_o(\Delta R)}{T_1(\Delta R)}\right] \frac{\pi}{2\Delta R} \frac{\alpha_1(T_o)}{S_1(T_o)} \frac{T(R)}{T_o} \frac{P(R)}{P_o} \exp\left[\frac{E_1}{k}\left(\frac{1}{T_o} - \frac{1}{T(R)}\right)\right] \quad . \tag{12}$$

Since the linewidth is a function of pressure, the accuracy of N(R) is dependent on an assumed value for P(R). However, by using the ideal gas law, $PV = nRT$, an accurate representation for the water vapor mixing ratio independent of P(R) can be written:

$$q(R) = \ln\left[\frac{T_o(\Delta R)}{T_1(\Delta R)}\right] \frac{\pi}{2\Delta R} \frac{\alpha_1(T_o)}{S_1(T_o)} \frac{T^2(R)}{T_o} \frac{R}{P_o} \exp\left[\frac{E_1}{k}\left(\frac{1}{T_o} - \frac{1}{T(R)}\right)\right] \quad . \tag{13}$$

where $\mathcal{R}$ is the ideal gas constant, and q(R) is the average water vapor mixing ratio in the range cell ΔR.

D. Transmission Characteristics

Using the AFGL line compilation data and the computer codes FSCDATM and FASCOD1, numerical calculations of the transmission for radiation in the region of 735 nm were performed. This work assumes atmospheric models to simulate the principles used in the DIAL technique. Figure 2 shows the one-way transmission spectrum from 13,600 to 13,630 cm^{-1} through a vertical 300-m column of 1962 U.S. Standard Atmosphere (at 284 K). The absorption in this region is due solely to water vapor lines. The DIAL temperature measurement technique described in the last section utilizes two of the lines in the region, 13,602 cm^{-1} and 13,628 cm^{-1}.

Figures 3 and 4 demonstrate the temperature dependence in the water vapor lines in this particular spectrum.

Individually, Figure 5 shows the change in the transmission profile with respect to temperature for the line at 13,602.63 cm^{-1}; Figure 6, for the line at 13,628.88 cm^{-1}. Note that the temperature dependence of these two lines is inversely related. Although the absorption strength of the two lines is comparable a the standard measurement temperature of 296 K, dissimilar ground-state energies for each of the lines (920.169 cm^{-1} for 13,602.631 and 23.794 cm^{-1} for 13,628.866) implies a large differential change in absorption with an increase or decrease in ambient temperature.

Figure 7 represents the change in transmission at line center for three wavelengths when the temperature in a range cell of 300 m varies from 254 to 314 K. As an implementation of the DIAL technique described in Section III.C, λ_o (the reference wavelength) is chosen to be 734.4 nm; λ_1 and λ_2 would then correspond to the two absorbing lines at 733.9 and 735.1 nm.

E. Alexandrite Laser Source

DIAL applications require precise tuning of the laser transmitter's wavelength output. The wavelength needs to be controlled to coincide with narrow absorption lines that correspond to the molecular resonances to be studied. Alexandrite is the only solid-state laser medium that is continuously tunable over a broad spectrum in the near-infrared, 720- to 790-nm (Walling et al., 1980).

Allied Chemical Corporation has patented a process to grow pure alexandrite crystal rods synthetically. This material exhibits similar high efficiency, high average power, and short pulse duration as other solid-state laser media, e.g., YAG and ruby. In essence, the design of an alexandrite laser resembles that used for YAG laser rods (Koechner, 1976). Thus, the reliability, ruggedness, compactness, and ease of

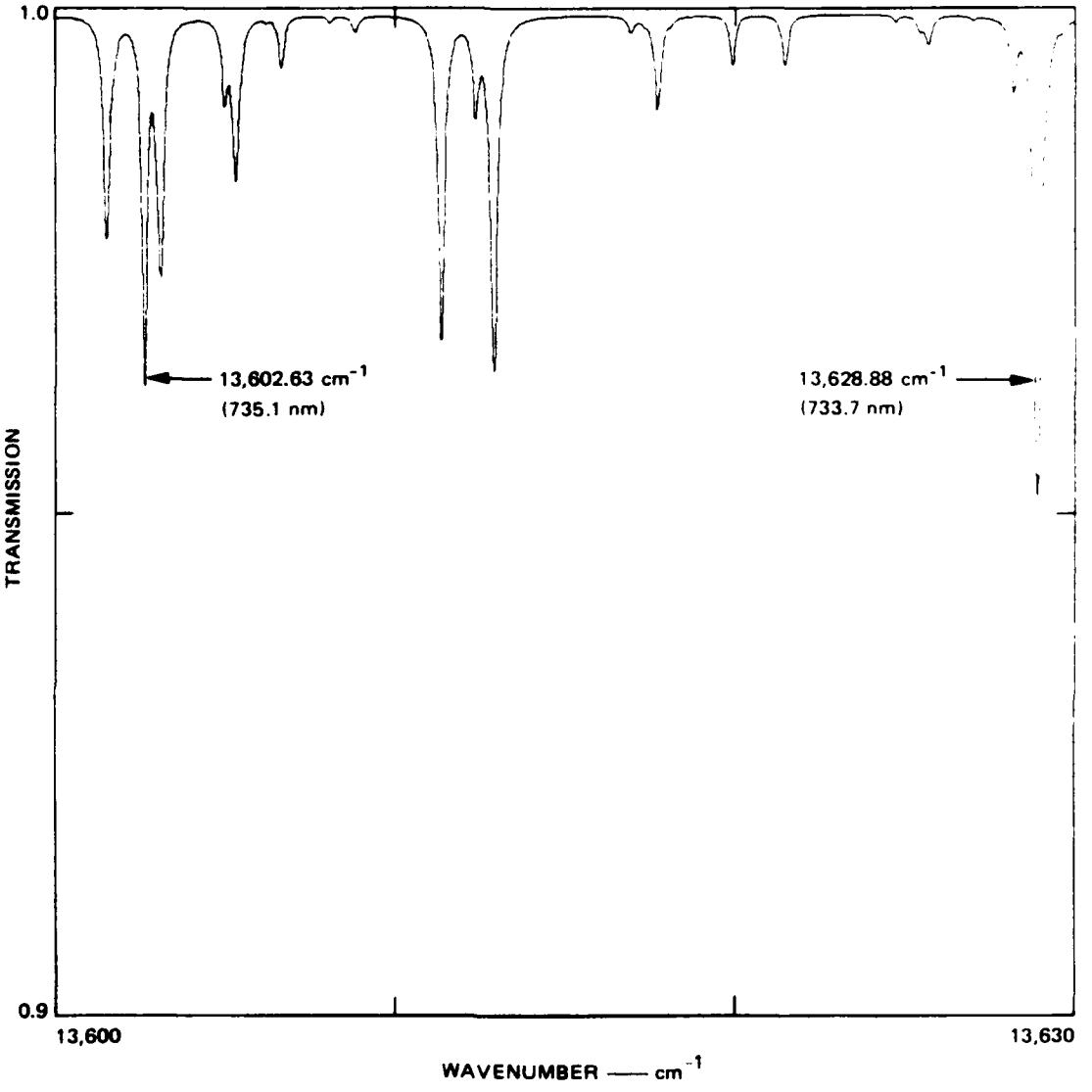

FIGURE 2 ONE-WAY TRANSMISSION SPECTRUM FROM 13,600 TO 13,630 cm^{-1} THROUGH 300 m OF 1962 U.S. STANDARD ATMOSPHERE AT 284 K

All absorption lines in this region are due to water vapor.

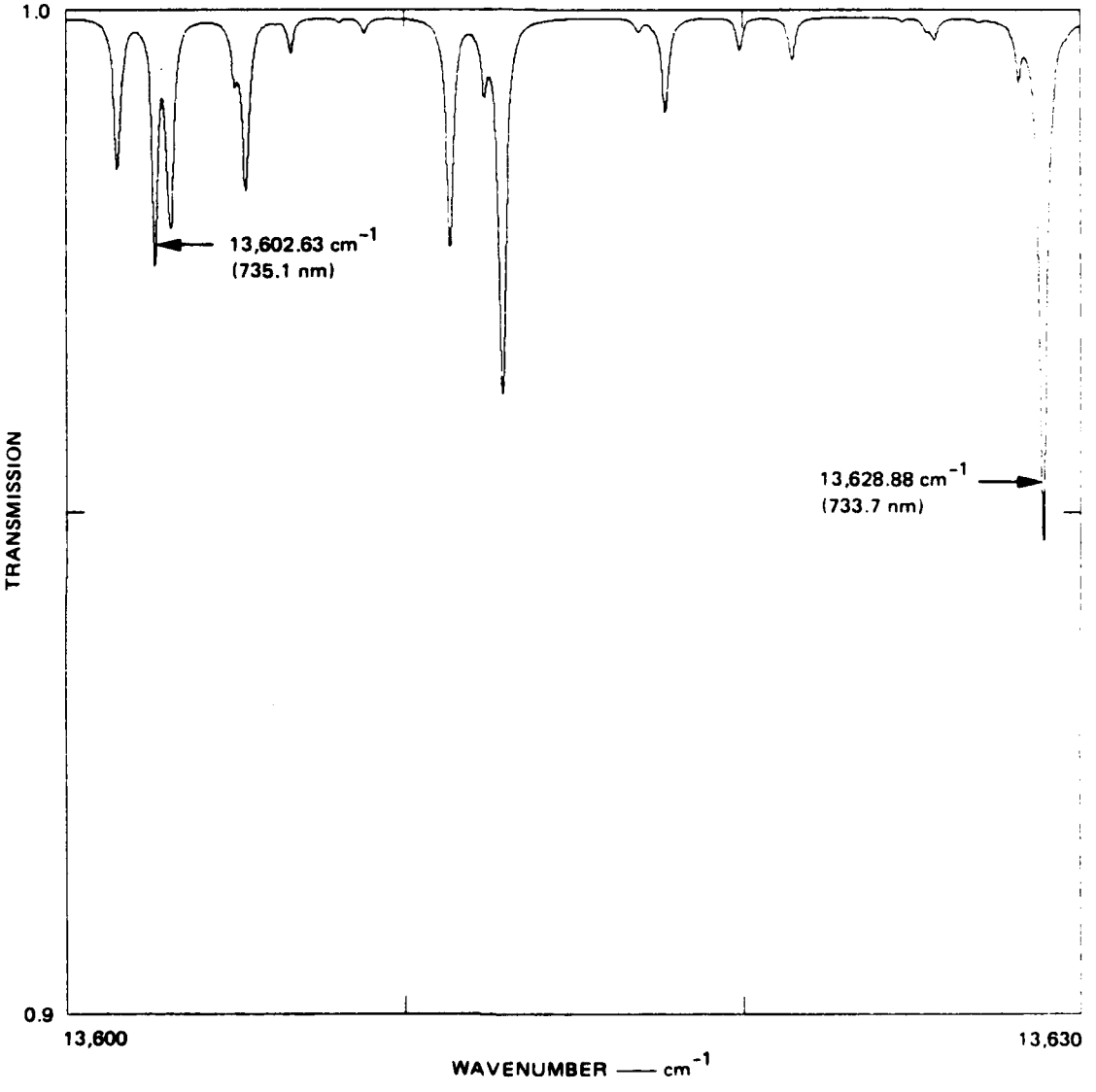

FIGURE 3 ONE-WAY TRANSMISSION SPECTRUM THROUGH 300 m OF 1962 U.S. STANDARD ATMOSPHERE AT 254 K

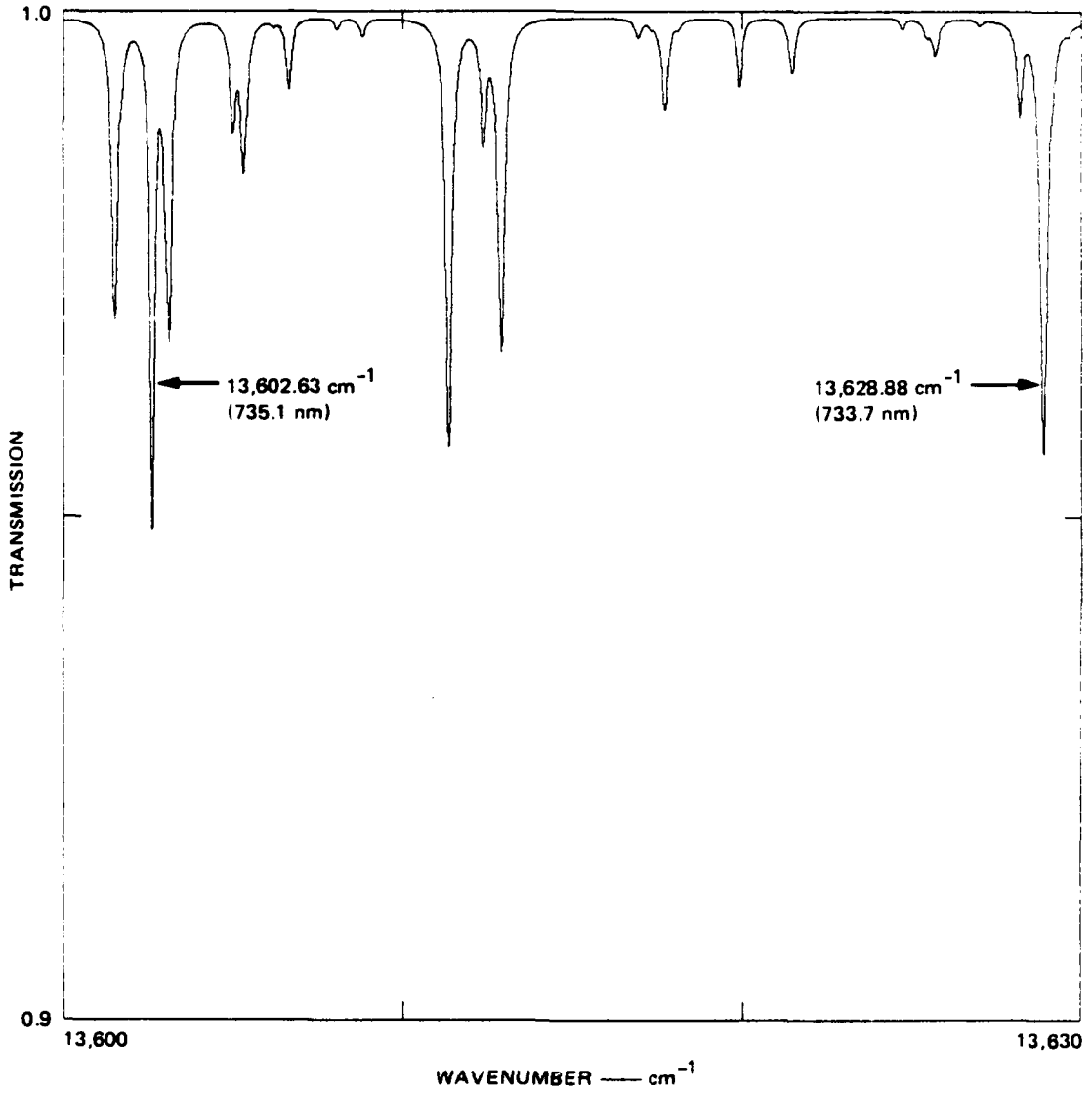

FIGURE 4 ONE-WAY TRANSMISSION SPECTRUM THROUGH 300 m OF 1962 U.S. STANDARD ATMOSPHERE AT 314 K

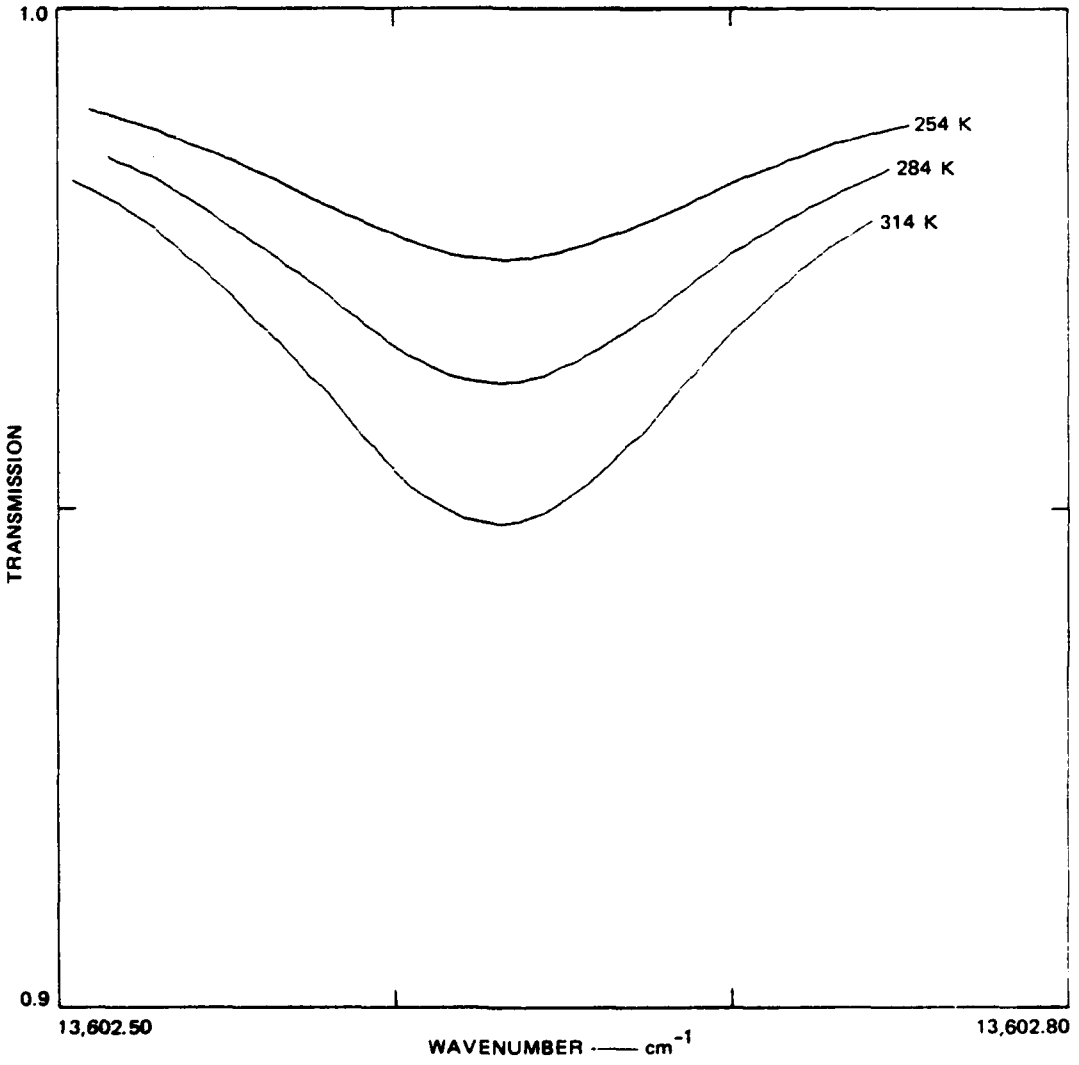

FIGURE 5 TRANSMISSION LINE PROFILES AT THREE TEMPERATURES FOR WATER VAPOR LINE CENTERED AT 13,602.63 cm^{-1}

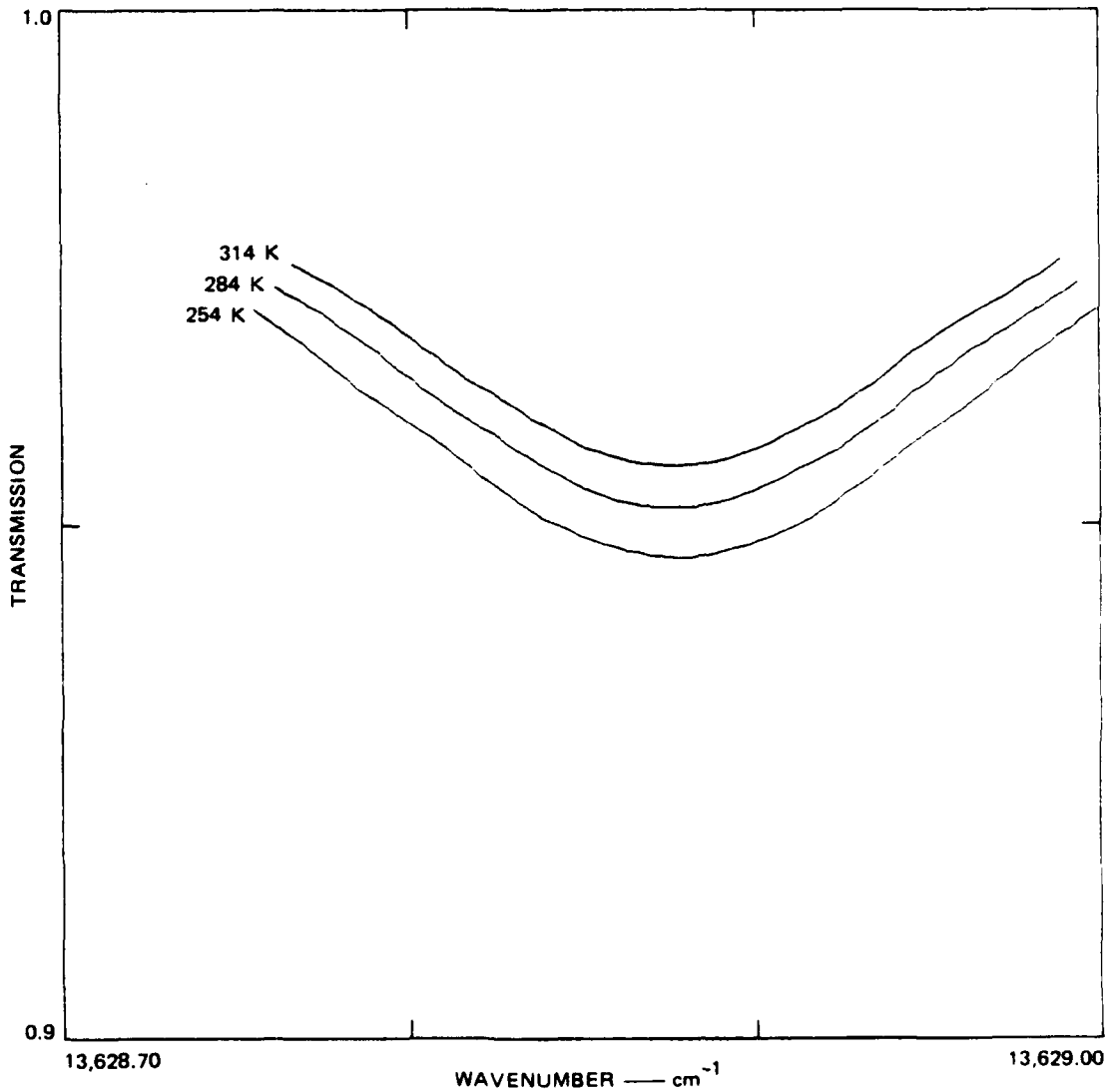

FIGURE 6 TRANSMISSION LINE PROFILES AT THREE TEMPERATURES FOR WATER VAPOR LINE CENTERED AT 13,628.88 cm^{-1}

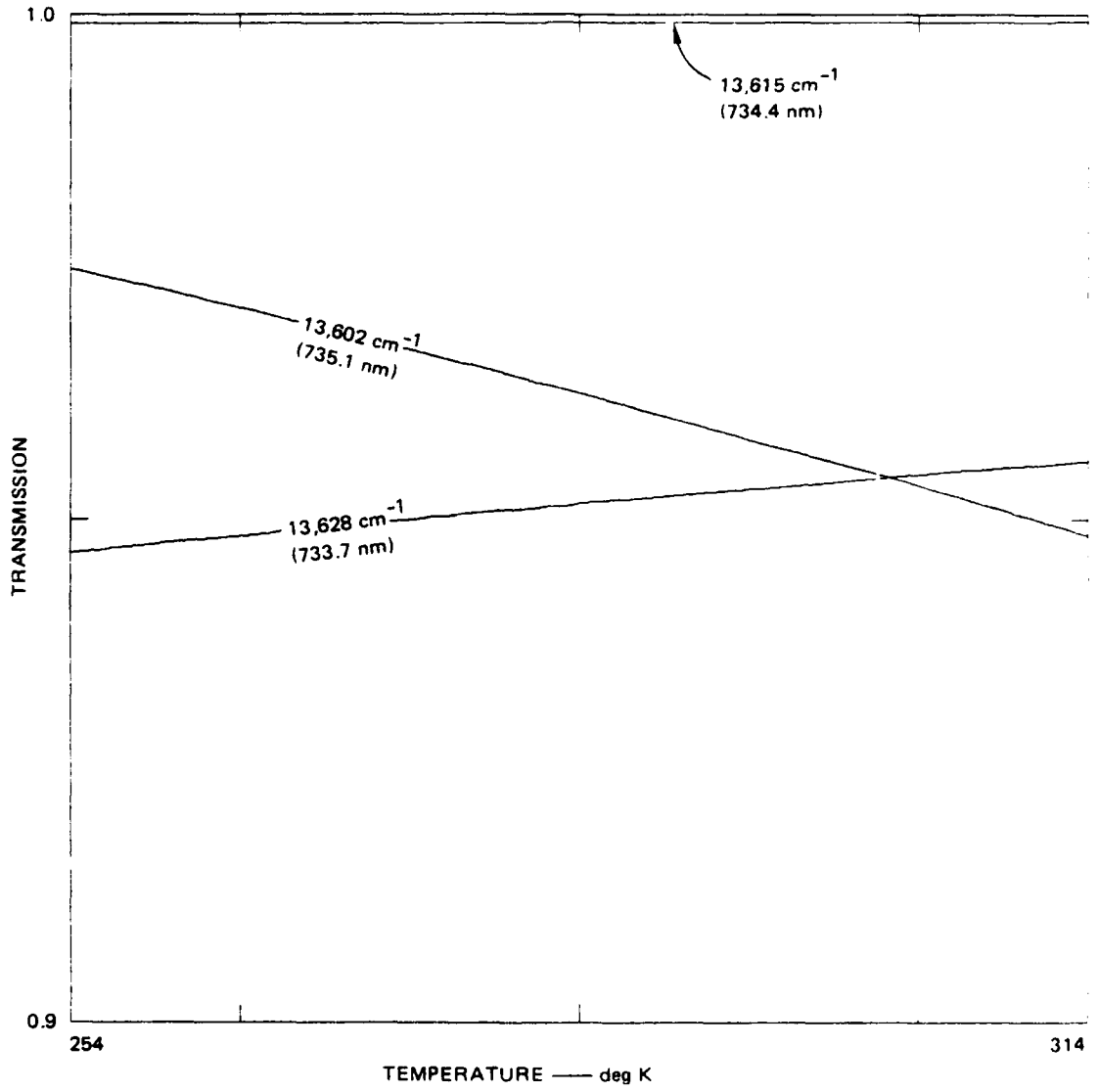

FIGURE 7 TEMPERATURE DEPENDENCE OF TRANSMISSION AT LINE CENTER FOR THREE WAVENUMBERS USED WITH THE DIAL WATER VAPOR AND TEMPERATURE TECHNIQUE

operation (excellent thermal conductivity allows room temperature operation) of a solid-state laser is available with a spectral output that is generally accessible only with dye lasers (which are usually pumped by solid-state lasers). The alexandrite laser medium operates as ruby except that the terminal lasing level is a band of vibrational energy states; these yield its primary tuning range (Walling, 1982). This tuning range can be continuously and rapidly scanned. Figure 8 shows the typical output energy available as a function of the laser's main tuning range.

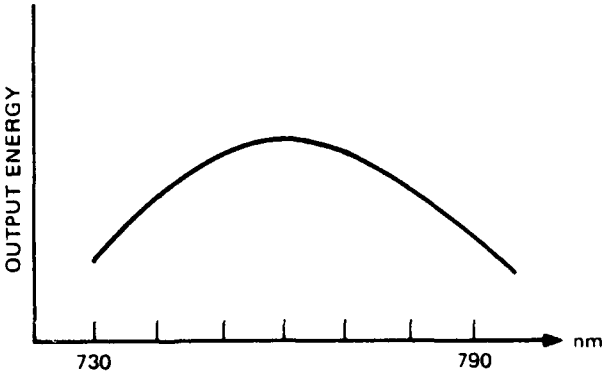

FIGURE 8 TYPICAL ENERGY OUTPUT OF THE ALEXANDRITE LASER (AT ROOM TEMPERATURE OPERATION) AS A FUNCTION OF OUTPUT WAVELENGTH TUNING

Figure 9 is a general schematic containing the major elements of a pulsed alexandrite laser. A pockels cell performs the Q-switching operation necessary for narrow pulsed outputs. The birefringent tuner controls the coarse continuous wavelength tuning. Intracavity etalons regulate fine tuning of the wavelength and the linewidth of the output pulse (Sam and Roukard, 1982).

Table 4 lists the specifications of an alexandrite laser that are commercially available. These capabilities justify the use of the alexandrite laser as a DIAL transmitter. For most of the items, improvement through an arrangement with the manufacturer during construction of the laser can be achieved.

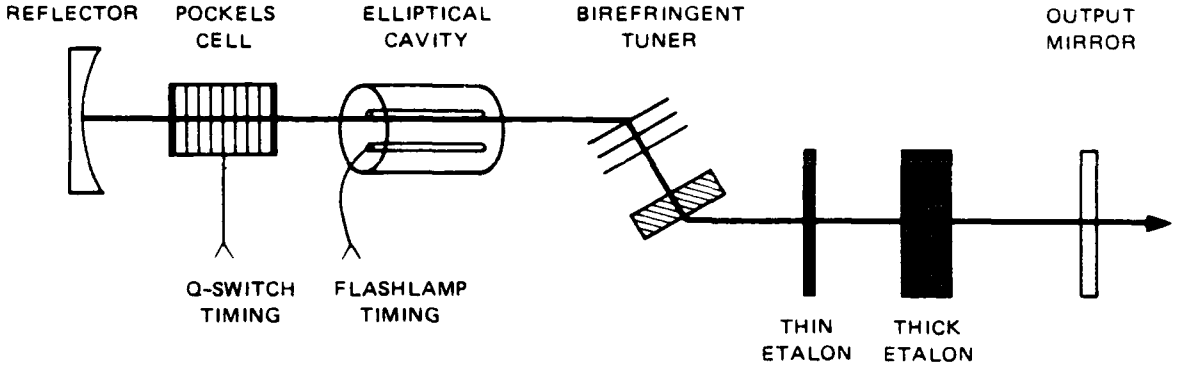

FIGURE 9 GENERAL SCHEMATIC OF A PULSED, WAVELENGTH TUNABLE ALEXANDRITE LASER

Table 4

ALEXANDRITE LASER OUTPUT SPECIFICATIONS

Wavelength (nm)	720-790
Energy (mj/pulse)	100
Maximum repetition rate (Hz)	10
Linewidth (nm)	.005
Beam divergence (mrad)	2

SUMMARY AND RECOMMENDATIONS

A. Results

A study and review of experimental systems using the DIAL and Raman remote systems techniques indicate that a DIAL system should be constructed to obtain ground-based vertical water vapor and temperature measurements for the removal of certain meteorological system errors from astronomical observations. This DIAL technique relies on a laser system that transmits high energy pulses at three specific wavelengths in the infrared spectrum.

Such DIAL systems have typically used dye lasers (optically pumped from another laser source, e.g., YAG) for study in the 700- to 800-nm wavelength region. However, the alexandrite solid-state material, which lases with continuous tunability in the same spectral region, offers several advantages:

- Chemical stability and physical durability.
- Simple Q-switching for narrow pulse widths because of strong polarized output from the crystal.
- Improved output energies and efficiency.
- Tuning by a low-loss quartz birefringent crystal and intracavity etalons.

Mass production of alexandrite rods has only recently been accomplished, and they are available only from a single supplier. (An alexandrite laser system can be purchased from the Military Laser Systems Division of Allied Chemical Corporation.) Experiments performed over the last two years at a number of research institutions indicate that it will be a significant laser source.

The alexandrite laser can be built into an optical and data collection system that will collect differential absorption data and store the results on magnetic tape for later analysis. Temperature and humidity values should also be collected simultaneously by the data system from in-situ sensors near the viewing path. Processing of the correction algorithms from atmospheric data does not require a "real-time" capability.

The absorption data obtained from the DIAL system will be translated into estimates of humidity and temperature. Correlative comparisons and checking of the validity of results can then be made with the in-situ sensors.

The DIAL technique has been successfully applied in the 724-nm wavelength region to obtain absolute humidity measurements. Also, DIAL remote temperature measurement systems with infrared laser sources have used oxygen lines near 760 nm (Mason, 1975; Schwemmer and Wilkerson, 1979). However, to provide simultaneous humidity and temperature measurements, the temperature dependence of water vapor lines near 734 nm needs to be utilized. The suggested DIAL temperature measurement technique uses the line strength dependence of the absorption lines centered near 735 nm and 733 nm. The absorption line at 735 nm deepens with increasing temperature; the line at 733 nm absorbs less with increasing temperature. By measuring this differential change in absorption, an estimate of the absolute temperature can be calculated. Thus, to obtain simultaneous temperature and humidity measurements, a three-wavelength DIAL system is needed; a two-wavelength system can provide only temperature or humidity results.

Figure 10 shows the optical components needed for the DIAL system. As shown, three laser sources will fire sequentially with 200 μs separation between pulses. The short inter-pulse time minimizes the temporal difference in the atmosphere that each pulse could encounter. The three beams are combined with beam splitters with a small portion of the energy removed and measured by a photo-multiplier tube (PMT) as a transmit energy monitor. The combined beams are then emitted through the center of the receiver telescope, allowing common optical alignment between the transmitted and received beams. The receiver's field of view is slightly larger than the transmitted beam divergence so that a slight error in alignment can be allowed. Direction of the optical beams is controlled vertically by a rotating mirror and horizontally by a dome that can be rotated.

The backscattered signals are collected and focused onto a second PMT that measures the received signal strength. Signal amplification in PMTs is accomplished by the conversion of photons to electrons by multiple grids within the unit. An optical conversion efficiency of 20 percent can easily be achieved. Typically, the electronic noise level output of the detector is lower than the background optical signal due to solar scattering during daytime operation. (The use of narrow bandwidth optical interference filters centered at the transmitted wavelengths minimize this background radiation level.)

The received signal is sampled and digitized [with a high-speed (20 MHz) 10-bit analog-to-digital (A-to-D) converter] and stored in the local data collection system. The receiver electronics, consisting of a linear amplifier and A-to-D converter, produces a representation of the returns with an accuracy of .1 percent over a range of three decades in magnitude. A sampling interval of 50 nsec allows a range resolution of 7.5 m along the optical path.

By measuring the time delay from the laser firing until the pulse reaches a region of interest and returns, the specific backscattered strength of one of the transmitter wavelengths can be obtained. Even though

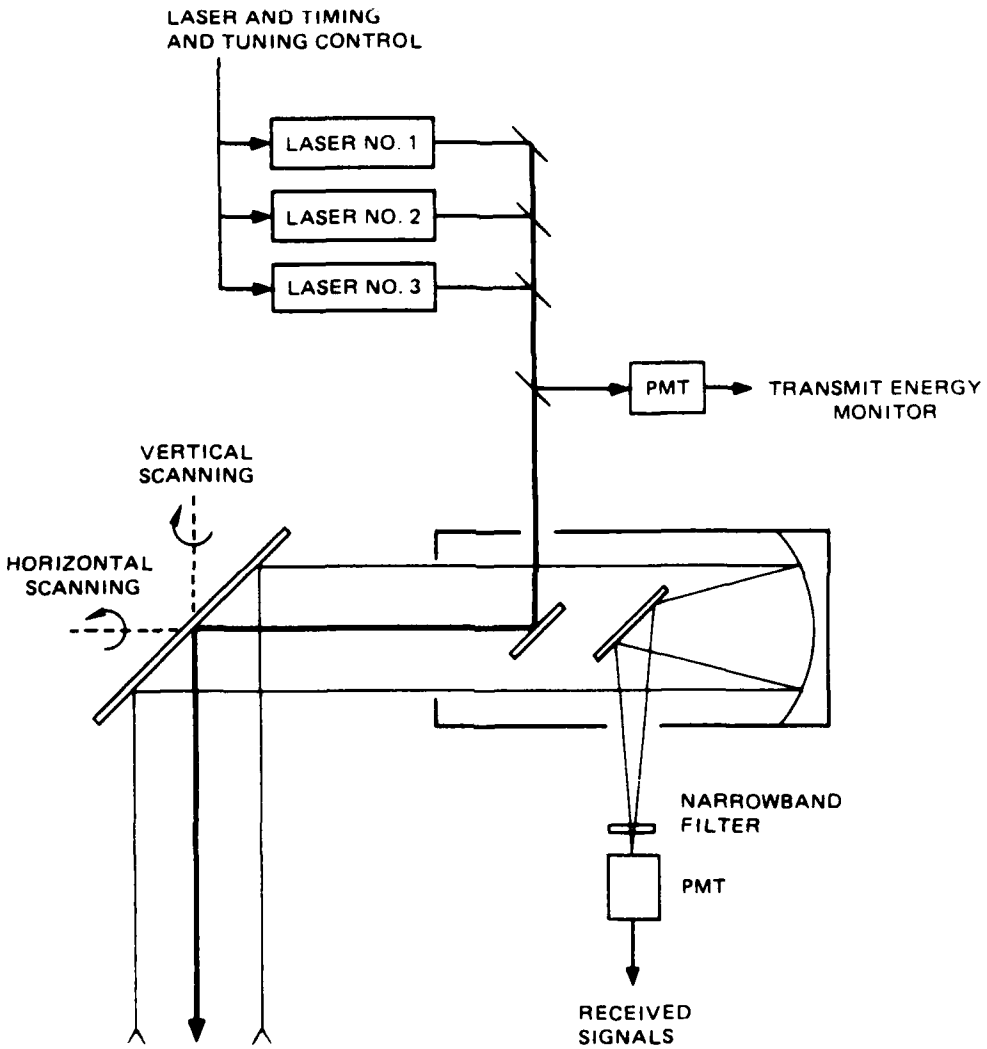

FIGURE 10 OPTICAL SCHEMATIC FOR SCANNING DIAL SYSTEM

a single receiver channel is used to measure data for all three wavelengths, specific wavelength backscatter in the received waveform can be selected by the controlled inter-pulse time of the laser transmitters. With this information the DIAL processing equations for temperature and water vapor density can be utilized during off-line processing, and a range profile can be estimated.

B. Recommendations

Two major atmospheric measurement problems for compensation of distortion in ground-based astronomical imaging are the vertical profile of water vapor and the distribution of temperature from ground level to a height of a few kilometers. The suggested remote sensing lidar system is designed specifically to obtain simultaneous data of these two quantities. It consists of a three-wavelength laser source and subsequent DIAL analysis of the range-resolved backscattered signals.

The technique for temperature measurement employs all three wavelengths, two of which are tuned to water vapor absorption lines (near 734 nm) and one nonabsorbing reference wavelength. Water vapor content can be obtained with a DIAL analysis of either of the two absorbing wavelengths and the reference wavelength.

Alexandrite should be employed as the lasing medium for the lidar system, allowing ease of operation, solid-state ruggedness, and reliability. The laser is continuously tunable from 720 nm to 790 nm, covering an important spectral region for water vapor absorption. (For the three-wavelength method at 734 nm, two of the wavelengths should be controlled to within .005 nm and the other to within .1 nm.) This system also has the capability to study other techniques in the infrared, including water vapor absorption measurements at 724 nm and temperature and density measurements at 760 nm using oxygen absorption lines.

Before a system can be directly applied to studying astronomical refraction at the Naval Observatory in Washington, D.C., a breadboard should be constructed with two alexandrite lasers. The primary goals for the breadboard system would be: (1) characterization and operational experience with the alexandrite lasers, and (2) application and subsequent analysis of the DIAL technique for obtaining water vapor profiles. A third laser and conical-scanning optics would then be added to include simultaneous temperature distribution and isothermal tilt measurements. The results of the complete breadboard project would demonstrate the functional aspects of the alexandrite DIAL system for the remote sensing of water vapor and temperature.

V REFERENCES

Browell, E.V., A.F. Carter, and T.D. Wilkerson, 1981: "Airborne Differential Absorption Lidar System for Water Vapor Investigations," Opt. Eng., Vol. 20, pp. 84-90.

Browell, E.V., T.D. Wilkerson, and T.J. McIlrath, 1979: "Water Vapor Differential Absorption Lidar Development and Evaluation," Appl. Opt., Vol. 18, pp. 3474-3483.

Cahen, C., and J.L. Lesne, 1981: "Improvements to Water Vapor Lidar Using DIAL Technique," Proc. Conf. Lasers and Electro-Optics, Washington, D.C.

Cahen, C., J. Pelon, P. Flamant, J. LeFrere, M.L. Chanin, and G. Megie, 1980: "French Lidar Facility at the Haute Province Observatory for Tropospheric and Stratospheric Measurements," Proc. Tenth Int. Laser Radar Conf., Silver Spring, Maryland.

Clough, S.A., and F.X. Kneizys, 1979: "Convolution Algorithm for the Lorentz Function," Appl. Opt., Vol. 18, pp. 2329-2333.

Cooney, J., and M. Pina, 1976: "Laser Radar Measurements of Atmospheric Temperature Profiles by Use of Raman Rotational Backscatter," Appl. Opt., Vol. 15, pp. 602-603.

Cooney, J., 1970: "Remote Measurements of Atmospheric Water Vapor Profiles Using the Raman Component of Laser Backscatter," J. Appl. Met., Vol. 9, pp. 182-184.

Endemann, M., and R.L. Byer, 1981: "Simultaneous Remote Measurements of Atmospheric Temperature and Humidity Using a Continuously Tunable IR Lidar," Appl. Opt., Vol. 20, pp. 3211-3217.

Endemann, M., and R.L. Byer, 1980: "Remote Single-Ended Measurements of Atmospheric Temperature and Humidity at 1.77 μm Using a Continuously Tunable Source," Opt. Letters, Vol. 5, pp. 452-454.

Gill, R., K. Geller, J. Farina, and J. Cooney, 1979: "Measurement of Atmospheric Temperature Profiles Using Raman Lidar," J. Appl. Met., Vol. 18, pp. 225-227.

Hake, Jr., R.D., W.B. Grant, and N. Cianos, 1977: Comparison of Lidar Techniques for Measuring Atmospheric Water-Vapor Concentrations, Report No. NADC 76149-20, SRI International, Menlo Park, California.

Hinkley, E.D. (ed.), 1976: Laser Monitoring of the Atmosphere, Springer-Verlag, New York.

Kalshoven, J.E., Jr., C.L. Korb, G.K. Schwemmer, and M. Dombrowski, 1981: "Laser Remote Sensing of Atmospheric Temperature by Observing Resonant Absorption of Oxygen," Appl. Opt., Vol. 20, pp. 1967-1971.

Koechner, W., 1976: Solid-State Laser Engineering, Springer-Verlag, New York.

Lebow, P., S. Strobel, T. Wilkerson, L. Cotnoir, and A. Rosenberg, 1982: "Remote Laser Measurement of Temperature and Humidity Using Differential Absorption in Atmospheric Water Vapor," Proc. Eleventh Int. Laser Radar Conf., Madison, Wisconsin.

Mason, J.B., 1975: "Lidar Measurement of Temperature: A New Approach," Appl. Opt., Vol. 14, pp. 76-78.

McClatchey, R.A., et al., 1973: AFCRL Atmospheric Absorption Line Parameters Compilation, Report No. TR-73-96, Air Force Cambridge Research Laboratories, Bedford, Massachusetts.

McClatchey, R.A., et al., 1970: Optical Properties of the Atmosphere, Report No. AFCRL-70-0527, Air Force Cambridge Research Laboratories, Bedford, Massachusetts.

Melfi, S.H., 1972: "Remote Measurements of the Atmosphere Using Raman Scattering," Appl. Opt., Vol. 11, pp. 1605-1610.

Pourny, S.C., D. Renault, and A. Orszag, 1979: "Raman-Lidar Humidity Sounding of the Atmospheric Boundary-Layer," Appl. Opt., Vol. 18, pp. 1141-1148.

Renault, D., J.C. Pourny, and R. Capitin, 1980: "Daytime Raman-Lidar Measurements of Water Vaopr," Opt. Let., Vol. 5, pp. 233-235.

Rosenberg, A., and D.B. Hogan, 1981: "Lidar Technique of Simultaneous Temperature and Humidity Measurements: Analysis of Mason's Method," Appl. Opt., Vol. 20, pp. 3286-3288.

Rothmann, L.S., et al., 1981: "AFGL Trace Gas Compilation: 1980 Version," Appl. Opt., Vol. 20, pp. 1323-1328.

Rothmann, L.S., 1980: "AFGL Atmospheric Absorption Line Parameters Compilation: 1980 Version," Appl. Opt., Vol. 20, pp. 791-795.

Sam, R.C., and F.P. Roukard, III, 1982: "Narrow Band, Tunable Alexandrite for Meteorological LIDAR," Electro-Optical Sys. Des., July 1982, pp. 37-40.

Schwemmer, G.K., and T.D. Wilderson, 1979: "Lidar Temperature Profiling: Performance Simulations of Mason's Method," Appl. Opt., Vol. 18, pp. 3539-3541.

Shotland, R.M., 1974: "Errors in the Lidar Measurement of Atmospheric Gases by Differential Absorption," J. Appl. Met., Vol. 13, pp. 71-77.

Smith, H.J.P., et al., 1978: FASCODE - Fast Atmospheric Signature Code (Spectral Transmittance and Radiance), Report No. AFGL-TR-78-0081, Air Force Geophysics Laboratory, Hanscom AFB, Massacusetts.

Walling, J.C., 1982: "Alexandrite Lasers: Physics and Performance," Laser Focus, February 1982, pp. 45-50.

Walling, J.C., O.G. Petersen, H.P. Jenssen, R.C. Morris, and E.W. O'Dell, 1980: "Tunable Alexandrite Lasers," IEEE J. Quan. Elec., Vol. QE-16, pp. 1302-1315.

Werner, C., and H. Hermann, 1981: "Lidar Measurements of the Vertical Absolute Humidity Distribution in the Boundary Layer," J. Appl. Met., Vol. 20, pp. 476-481.

Wilkerson, T.D., G. Schwemmer, B. Gentry, and L.P. Giver, 1979: "Intensities and N_2 Collision-Broadening Coefficients Measured for Selected H_2O Absorption Lines Between 715 and 732 nm," J. Quant. Spec. Rad. Trans., Vol. 22, pp. 315-331.

Wright, M.L., E.K. Proctor, L.S. Gasiorek, and E.M. Liston, 1975: A Preliminary Study of Air-Pollution Measurement by Active Remote-Sensing Techniques, Report No. NASA CR-132724, SRI International, Menlo Park, California.

Appendix

THE USE OF LIDAR TO OBTAIN THREE-DIMENSIONAL REFRACTION DATA*

*Paper presented at the Sixth European Astronomical Meeting, Belgrade, Yugoslavia (October 1981).

THE USE OF LIDAR TO OBTAIN THREE-DIMENSIONAL REFRACTION DATA

J.A. Hughes
U.S. Naval Observatory, Washington, DC

S. DeLateur
SRI International, Menlo Park, CA

Abstract: The need for a real time (or near real time) detailed knowledge of the atmospheric structure necessary for determining astronomical refraction in general is exhibited. Examples involving water vapor and isopycnic tilts are given.

The possibility of determining the necessary parameters by means of active atmospheric probing using Light Detection and Ranging (Lidar) methods is reviewed. A brief discussion of Raman versus Differential Absorption Lidar (DIAL) techniques is included. Recent advances in applicable lasing materials such as the Alexandrite crystal offer interesting possibilities.

At the present time a conceptual design study is underway. This is intended to culminate in the construction of a system in 1982-83.

INTRODUCTION

The most exasperating characteristic of astronomical refraction is the fact that while it is a relatively straight-forward matter to account for nearly 99.9% of the effect, it is currently essentially impossible to allow for the remaining 0.1% with any assurance of success. We have however, reached the point where that remaining 0.1% is important, and especially so if any part of it is systematic. This situation is not caused by a lack of excellent theories of refraction. We have the Pulkovo Tables (1956) and Garfinkel's (1967) polytropic theory to name but two of the prominent methods available. The problem is that it is just too much to expect any theory, even one with many adjustable parameters, to account for the minute by minute or even hourly variations in the dynamic planetary boundary layer. On the whole it is noteworthy how well the theories succeed since they are essentially static representations of the atmosphere.

WATER VAPOR

Consider the effect of water vapor. It changes both the refractivity and the gas constant so as to decrease the refraction. Difficulties

arise when one uses only a ground level value of the humidity without any knowledge of the actual three dimensional distribution of the water vapor. Merely using the observed ground level value of the ratio of the partial pressure of water vapor to the total pressure, Pw/Pt, is equivalent to assuming that this ratio is a constant throughout the atmosphere. Since humidity falls rapidly with height this procedure would generally overestimate the effect of the water vapor.

In order to illustrate this type of problem the changes in refraction (with respect to dry air) caused by various partial pressures of water were computed using the Pulkovo Tables (IV ED.), and also by means of numerical integrations of various water vapor profiles. The differences in the changes using these two methods were then computed and tabulated. For a total ground level pressure near 760 mm Hg, with 10 mm being due to water vapor, and for temperatures in the range of 273° to 293° K, it was found that good agreement occurred when the water vapor was assumed to decline linearly with height, reaching zero at seven kilometers. Table I illustrates these differences, Change (Integration) - Change (Pulkovo), for that profile. Evidently if one happened to be observing under just the right conditions, a near perfect allowance for water vapor would be made. However, as Table I shows, the differences become greater at lower total pressures or higher partial pressures of water vapor. There is, in addition, no guarantee that the true profile is that which was assumed here.

TABLE I

Change (Integration) - Change (Pulkovo)

T°K / Pt mm	273		283		293	
	Pw = 10	Pw = 30	Pw = 10	Pw = 30	Pw = 10	Pw = 30
760	-.001	-.014	-.001	-.012	-.002	-.013
640	+.017	+.045	+.018	+.042	+.017	+.042
560	+.032	+.084	+.030	+.081	+.029	+.079

ISOPYCNIC TILT

A second contributor to the types of error considered here is any systematic tilt of the assumed isopycnics. One of us, Hughes (1979), has done considerable theoretical work on the generation of such tilts by urban heat islands. Without going into great detail we present here two cross sections through the density perturbation field caused by a realistic heat island. Cross section A lies in the plane of the meridian of a hypothetical observatory, while section B lies in the plane of the corresponding prime vertical. Table II shows the values of the tilt angles in these planes. The observatory is supposed to be located some 6 km southeast of the center of the heat island. The wind is assumed to

be from the west. Values are given up to a height of 500 m and for horizontal distances of 400 m and 800 m (negative to the south for section A and to the west for section B).

TABLE II
Isopycnic Tilts

	Section A					Section B				
Meters	-800	-400	0	+400	+800	-800	-400	0	+400	+800
100	$+.^{\circ}04$	$+.^{\circ}09$	$+.^{\circ}15$	$+.^{\circ}21$	$+.^{\circ}25$	$+.^{\circ}43$	$+.^{\circ}42$	$+.^{\circ}41$	$+.^{\circ}39$	$+.^{\circ}37$
200	+.11	+.10	+.08	+.05	+.02	+.14	+.11	+.08	+.06	+.03
300	-.02	-.04	-.05	-.06	-.06	-.08	-.09	-.10	-.10	-.09
400	-.05	-.05	-.04	-.03	-.02	-.11	-.09	-.08	-.06	-.05
500	-.01	-.00	+.01	+.01	+.01	-.03	-.01	+.00	+.01	+.01

These results are strictly theoretical, and although the order of magnitude of the tilts is reasonable, there is no guarantee that the true tilt is that which is shown here.

Thus for the two phenomena considered above we are presently forced into what are essentially ad hoc assumptions and procedures. This unsatisfactory situation can only be improved by injecting additional, real time, three dimensional atmospheric data into the various algorithms used for treating observational material.

LIDAR

One method of generating the required data is with a laser detection and ranging (Lidar) system. The approach is similar to conventional radar, except the interactions occur at optical frequencies. With the laser transmitter and receiver systems positioned at a common location, a telescopic optical receiver measures the amount of backscatter from a short transmitted laser pulse. Ranging is performed by calculating the time for the pulse to travel the distance to a region of interest plus the time for the backscattered pulse to return. Thus, by sampling the time-varying received optical intensity after a specific delay, study of a restricted location along the path can be accomplished.

By using models that describe the absorption and scattering properties of the atmosphere at optical frequencies, information about major and trace constituents can be obtained through "inverting" the measurements of backscattered intensity. Depending on the realm of study, the frequency of the transmitter, the frequency response of the receiving system, the optics design, and the data processing can be selected to provide a large area of coverage and rapid measurement capabilities. See Hinkley (1976) for an excellent review of the field.

DIAL AND RAMAN LIDAR SYSTEMS

Two different Lidar techniques will be discussed in this paper: (1) Differential Absorption Lidar (DIAL) and (2) Raman Lidar. Each of these are candidates as system approaches to provide vertical profiles of atmospheric water vapor content and temperature. However, the scattering and absorption basis for the measurements are distinct in each system.

The laser transmitter of the DIAL system sends pulses at two wavelengths. One wavelength is selected to coincide with an absorbing line of the molecular species of interest. The other near-by wavelength is chosen for negligible absorption. The receiving system is tuned to measure the elastic Mie and Rayleigh backscatter at the same wavelengths as were transmitted. By forming the difference of the returned intensities at the absorbed and unabsorbed wavelengths, a time-varying (and thus, range resolved) concentration of the species is estimated. This technique has also been called Differential Absorption of Scattered Energy (DASE) and Differential Absorption and Scattering (DAS).

The transmitter of a Raman Lidar system sends a pulse of a single wavelength. The receiver system is tuned to the wavelengths that are uniquely Raman-shifted (from the transmitted wavelength) by the molecular species to be studied. By using the Raman cross-section of the species, an analysis of the magnitude of the received intensity can be translated into a concentration profile.

WATER VAPOR MEASUREMENT SYSTEMS

Both Raman and DIAL systems are used successfully to obtain water vapor measurements. Only those experiments that have supplied vertical profiles are listed in the following tables; those systems that supply a column integrated measurement or average along a horizontal path are not included.

Table III shows the range of Raman systems that have been designed specifically for water vapor profiles. All of these systems fundamentally measure the ratio of the number density of H_2O to that of N_2. Thus, only a water vapor mixing ratio is estimated. This can be translated into a water vapor profile by assuming a density profile for N_2 with accompanying error.

Table IV lists recent water vapor profiling DIAL systems. Less powerful laser transmitters are typically needed than those used in Raman-based systems because the Rayleigh-Mie backscatter cross-sections are many orders of magnitude larger than Raman cross-sections.

TABLE III

Raman Lidar Systems for Vertical Water Vapor Profiling

Cooney (1971) Transmitter: doubled Ruby at 347.15nm. Receiver: 397.5 nm from H_2O and 377.7 nm from N_2. Approach: water vapor profile obtained by normalizing H_2O Raman return with N_2 return, and assuming an N_2 atmospheric content. 13 percent accuracy. Night measurement. Range: 300 m - 2600 m with 100 m intervals.
Melfi (1972) Transmitter: doubled Ruby at 347.15 nm. Receiver: 397.5 nm from H_2O and 377.7 nm from N_2. Approach: water vapor profile from H_2O return normalized by N_2 return. Night measurement. Range: 200 m - 2500 m with 50 m intervals.
Pourny, Renault, and Orszag (1979) Transmitter: doubled ruby at 347.15 nm. Receiver: 397.6 nm from H_2O and 377.7 nm from N_2. Approach: water vapor mixing ratio from H_2O return normalized by N_2 return. Night measurement. 15 percent accuracy. Range: 300 m - 1800 m with 30 m intervals.
Renault, Pourny, and Capitini (1980) Transmitter: quadrupled YAG at 266 nm. Receiver: 277.5 nm from O_2. 283.6 nm from N_2, and 294.6 nm from H_2O. Approach: water vapor mixing ratio from the H_2O return is normalized by the N_2 return. Estimation of ozone concentration is used to compensate for heavy ozone attenuation of the signals in this wavelength region. 10 percent accuracy at 500 m with 30 m intervals. Daytime operation. Range: 150 m - 950 m with 30 m intervals.

TABLE IV
DIAL Systems for Vertical Water Vapor Profiling

Browell, Wilkerson, and McIlrath (1979) Transmitter: ruby at 694.3 nm and dye (pumped by ruby) at 724.3 nm. Receiver: 724.3 nm (water vapor absorbing wavelength) and 694.3 nm. Approach: difference in returned signals is analyzed for H_2O density profile (mol/cm^3). Equipment includes an absorption cell that measures the cross-section for H_2O at the dye laser output for each pulse. 9 percent accuracy. Night operation. Range: 100 m - 3000 m with 100 - 180 m intervals.
Cahen, Pelon, Flamant, Lefere, Chanin, and Megie (1980); also, Cahen and Lesne (1981) Transmitter: Nd: YAG at 532 nm and dye (pumped by Nd:YAG) at 723 nm. Receiver: 723 nm (absorbed by water vapor) and 532 nm Approach: difference returns to obtain water vapor profiles. Wavelength and line-width are servo-controlled. 10 percent accuracy. Daytime operation. Range: 8000 m with 30 m intervals.
Werner and Herrmann (1981) Transmitter: ruby at 694.28 nm and temperature varied ruby from 694.2 nm to 694.28 nm. Receiver: 694.215 nm (absorbed by water vapor) and 694.237 nm. Approach: difference returns to obtain water vapor density profiles. Accuracy of 1 mbar in absolute humidity. Daytime operation. Range: 450 m - 1500 m with 100 m intervals.

TEMPERATURE PROFILING SYSTEMS

Table V contains a list of Raman temperature profiling systems. Common to these experiments is the technique of measuring the temperature dependence in the magnitude of the Raman spectrum of N_2 and O_2. The lines in the Raman spectrum have differential changes in magnitude with respect to temperature. Thus, by comparing the change in two bands, temperature value can be deduced.

There is a lack of DIAL vertical temperature profiling systems. However, work is presently being performed with system techniques that show promise. One proposal is to use "Mason's Method" (Mason, 1975. Schwemmer and Wilkerson, 1979) with the absorption spectra of O_2 in the region of 760 nm. This wavelength is close to the wavelengths selected in successful DIAL water vapor measurements (720 nm). Thus a single system could supply temperature as well as water vapor density.

TABLE V
Raman Lidar Systems for Vertical Temperature Profiling

Cooney and Pina (1976) Transmitter: ruby at 694.3 nm. Receiver: 689.0 nm and 691.2 nm Approach: measure the difference in the magnitude of the Raman spectrum of O_2 and N_2 in two bands which vary with temperature. Accuracy is 5 degrees C. Nighttime operation. Range: 600 m - 1100 m with 300 m intervals.
Gill, Geller, Farina, and Cooney (1979) Transmitter: ruby at 694.3 nm. Receiver: 691.6 nm and 689.0 nm. Approach: same as above. Accuracy is .85 degrees C. Range: 1300 m - 2300 m with 75 m intervals.

A COMBINATION SYSTEM

The combined DIAL technique mentioned above is now being researched. Typically, dye lasers have been used to cover the 650 nm - 790 nm region as transmitters for such simultaneous temperature and humidity measurement system studies. Besides covering the important absorption regions for H_2O and O_2, they are easily tuned to specific wavelengths. However, solid-state lasers have demonstrated an ease of operation and reliability that is important for day-to-day meteorological observations. Recently, a solid-state lasing material, Alexandrite, was developed for laser output from 700 nm - 815 nm. Thus, the characteristics of this material are being included within new DIAL system designs.

CONCLUSION

It appears that Lidar offers real possibilities with regard to providing input data for use in refining our current allowances for refraction. Water vapor profiling presents no problem, and temperature measurements certainly are feasible. Since for the small perturbations considered here, the Boussinesq approximation is valid, it follows that isopycnics follow isotherms. Thus temperature measurements are equivalent to density measurements, and with, for example, a conically steered laser beam, the isopycnic tilts can be determined.

If present plans hold, a system to accomplish these ends will be in operation within two years. The results should be of considerable interest.

Bibliography

Browell, E.V., T.D. Wilkerson, and T.J. McIlrath, (1979): "Water Vapor Differential Absorption Lidar Development and Evaluation," Appl. Opt., vol. 18, 3474-3483.

Cahen, C., J. Pelon, P. Flamant, J. LeFrere, M.L. Chanin, and G. Megie, (1980): "French Lidar Facility at the Haute Provence Observatory for Tropospheric and Stratospheric Measurements," Proc. Tenth Int. Laser Radar Conf., Silver Spring, Maryland.

Cahen, C., and J.L. Lesne, (1981): "Improvements to Water Vapor Lidar Using DIAL Techniques," Proc. Conf. Lasers and Electro-Optics, Washington, D.C.

Cooney, J., (1970): "Remote Measurements of Atmospheric Water Vapor Profiles Using the Raman Component of Laser Backscatter," J. Appl. Met., vol. 9, 182-184.

Cooney, J. and M. Pina, (1976): "Laser Radar Measurements of Atmospheric Temperature Profiles by Use of Raman Rotational Backscatter," Appl. Opt., vol. 15, 602-603.

Garfinckel, B. (1967): "Astronomical Refraction in a Polytropic Atmosphere," Astron, J., 72, pp. 235-254.

Gill, R., K. Geller, J. Farina, and J. Cooney, (1979): "Measurement of Atmospheric Temperature Profiles Using Raman Lidar," J. Appl. Met.,

Hinkley, E.D., (1976): Laser Monitoring of the Atmosphere, Springer-Verlag, New York.

Hughes, J.A. (1979): "Environmental Systematics and Astronomical Refraction II," IAU Sym.,No. 89, Refractional Influences in Astronomy and Geodesy, Ed. Tengstrom and Teleki, pp. 13, 25.

Mason, J.B., (1975): "Lidar Measurement of Temperature: A New Approach," Appl. Opt., vol. 14, 76-78.

Melfi, S.H., (1972): "Remote Measurements of the Atmosphere Using Raman Scattering," Appl. Opt., vol. 11, 1605-1610.

Pulkovo Refraction Tables (1956), Academy of Sciences Press, IV. Ed., Moscow.

Pourny, J.C., D. Renault, and A. Orszag, (1979): "Raman-Lidar Humidity Sounding of the Atmospheric Boundary-layer," Appl. Opt., vol. 18, 1141-1148.

Renault, D., J.C. Pourny, and R. Capitin, (1980): "Daytime Raman-Lidar Measurements of Water Vapor," Opt. Let., vol. 5, 233-235.

Schwemmer, G.C. and T.D. Wilkerson, (1979): "Lidar Temperature Profiling: Performance Simulations of Mason's Method," Appl. Op., vol. 18, 3539-3541.

Werner, C., and H. Herrmann, (1981): "Lidar Measurements of the Vertical Absolute Humidity Distribution in the Boundary Layer," J. Appl. Met., vol. 20, 476-481.

END
DATE
FILMED

July 9, 1983